Research Article

Sumama Nuthana Kalva*, Yahya Zakaria, Carlos A. Velasquez, and Muammer Koç

Tailoring the mechanical and degradation properties of 3DP PLA/PCL scaffolds for biomedical applications

https://doi.org/10.1515/rams-2025-0098
received November 04, 2024; accepted January 31, 2025

Abstract: In the realms of tissue engineering and 3D printing, tailoring scaffold mechanical characteristics and degradation rates is crucial for superior performance in a range of biomedical settings. This research explores the use of poly(lactic acid) (PLA) and poly(ε-caprolactone) (PCL) blends as feedstocks for fused deposition modeling. We fabricated filaments using five different PLA/PCL ratios (100/0, 70/30, 50/50, 30/70, and 0/100) and utilized them to fabricate test samples using a 3D printer. This study assesses how PCL influences the thermal, physicochemical, and printing properties of PLA. The introduction of PCL, which has a lower melting point and greater ductility compared to PLA, not only enhances printability but also adds flexibility and governs the degradation pace of the scaffolds. Fourier transform infrared spectroscopy analysis reveals that the chemical functional groups of PLA and PCL are quite similar, leading to significantly overlapping infrared bands in the blends. PLA (70%) exhibits a high elastic modulus (1.23 GPa) and maximum tensile strength (32.5 MPa), demonstrating that it maintains its rigidity and strength despite the substantial inclusion of PCL. Furthermore, an increase in PCL content correlates with a reduction in weight loss, indicating slower degradation rates in phosphate-buffered saline. Our results provide a deeper understanding of how PLA/PCL ratios affect scaffold properties, offering important insights for creating custom scaffolds that meet specific needs in tissue engineering applications.

*** Corresponding author: Sumama Nuthana Kalva,** Division of Sustainable Development, College of Science and Engineering, Hamad Bin Khalifa University, Doha, Qatar, e-mail: sunu43717@hbku.edu.qa
Yahya Zakaria: Core labs, Hamad Bin Khalifa University, Doha, Qatar, e-mail: yzakaria.science@gmail.com
Carlos A. Velasquez: Surgical Research Section, Innovation Unit, Hamad Medical Corporation, Doha, Qatar, e-mail: CVelasquez@hamad.qa
Muammer Koç: Division of Sustainable Development, College of Science and Engineering, Hamad Bin Khalifa University, Doha, Qatar, e-mail: mkoc@hbku.edu.qa

Keywords: PLA, PCL, 3DP, filaments, biomedical

1 Introduction

With the goal of creating biomaterials that resemble natural bone structures and characteristics to support tissue regeneration, bone tissue engineering has emerged as a potential area of research in regenerative medicine [1–3]. The need for innovative materials and fabrication methods that can satisfy medical requirements for biodegradability, biocompatibility, and affordable, on-demand customized design and manufacture has arisen from the sharp rise in the use of orthopedic implants. Implants should mimic the characteristics of actual bone as closely as possible regarding strength, hardness, chemical composition, rate of deterioration, biocompatibility in the physiological environment, *etc.* [4,5]. Most implants that are offered commercially are made of metals and metallic alloys, such as titanium, stainless steel, and Co–Cr alloys, because of their superior mechanical strength, biocompatibility, and advantageous corrosion resistance properties [6–9]. However, their long-term use often leads to challenges, including stress shielding, inflammatory responses, and difficulties with biodegradation, necessitating surgical removal in many cases. These limitations have spurred interest in alternative materials that can better mimic the dynamic properties of natural bone while addressing these shortcomings.

In this context, polymer-based materials have emerged as a promising alternative, offering the advantages of biodegradability, tunable properties, and ease of fabrication through advanced techniques like additive manufacturing [10–12]. Among these, poly(lactic acid) (PLA) [13–15] and poly(ε-caprolactone) (PCL) [16–18] stand out as two leading candidates for bone tissue engineering, owing to their biocompatibility, mechanical properties, and degradability profiles. This shift from metals to polymers marks a significant step forward in creating implants that integrate seamlessly into the physiological environment while minimizing complications.

Even though both PLA and PCL have shown promise for bone tissue engineering when used separately [19–22], their combination in polymeric blend materials can have beneficial synergistic effects and enhance performance. The combination of PLA and PCL enhances materials by leveraging PLA's stiffness and biodegradability alongside PCL's flexibility and slower degradation rate. The mechanical qualities, degradation rates, and bioactivity crucial for bone tissue regeneration can be adjusted by blending PLA and PCL [23,24]. Additionally, fused filament fabrication (FFF) has many benefits as an additive manufacturing method, including simplicity of usage, affordability, and the capacity to create patient-specific scaffolds with complex designs [25,26].

Although several studies have explored the properties of PLA/PCL blends, much of the existing literature focuses on either individual polymer characteristics or blends with fixed ratios. However, there is limited research that systematically evaluates how varying PLA/PCL ratios influence both mechanical and degradation properties, specifically in the context of 3D-printed scaffolds for bone tissue engineering. Furthermore, most studies do not address the processability challenges associated with these blends when used as feedstock for FFF. This study bridges these gaps by comprehensively analyzing the thermal, printing, mechanical, and degradation behaviors of 3DP PLA/PCL blends across a range of blend ratios.

2 Materials and methods

2.1 Materials

PLA particles were sourced from Goodfellow Cambridge Limited, characterized by an average molecular weight of 193,300 $g \cdot mol^{-1}$, melting point of approximately 170°C, and granule size ranging from 3 to 5 mm. The density of PLA was 1.24 $g \cdot cm^{-3}$, with a melt flow rate (MFR) of 8. PCL was purchased from Sigma Aldrich, possessing a melting point near 60°C, average molecular weight close to 80,000 $g \cdot mol^{-1}$, granule size around 3 mm, and a density of 1.145 $g \cdot cm^{-3}$. The MFR of PCL ranges from 2 to 4. Chloroform, used as a solvent for polymers, was obtained from VWR Chemicals (Germany) and has a density of 1.48 $g \cdot cm^{-3}$ and a boiling point near 60°C.

2.2 Preparation of PLA/PCL films

Films were produced with varying PLA/PCL blends using a solvent evaporation technique. Concentrations were set at 125 $g \cdot l^{-1}$ for each mixture with varying PLA/PCL ratios (100/0, 70/30, 50/50, 30/70, and 0/100). The mixtures were stirred mechanically at 400 rpm for 24 h at room temperature (Table 1). These solutions were then spread onto a standard-sized metal plate to air dry for 24 h before the film removal. The same size plate was used for consistency in the thickness of films.

2.3 PLA/PCL filament extrusion

Following film preparation, the PLA/PCL films were shredded into uniform squares to serve as extruder feedstock (Figure 1). The neat PLA and PCL filaments were extruded following our previous reports on PLA and PCL magnesium composites [18,27]. The Filabot EX2 extruder produced the filaments through a 3 mm nozzle. The PLA/PCL were found to be extrudable consistently at 160°C. The extruded PLA/PCL filaments were subjected to quality checks to ensure consistent performance during 3D printing. Diameter uniformity was measured using a digital caliper, ensuring the filament diameter remained within the acceptable tolerance range specified for the Ultimaker 3 Extended 3D printer (2.85 ± 0.05 mm). Additionally, cross-sectional analysis was performed visually to inspect the filaments for any air voids or inconsistencies that could compromise the mechanical integrity and printability of the material. These checks were critical for achieving smooth extrusion and ensuring structural uniformity in the printed scaffolds. These filaments were then utilized for 3D printing.

2.4 Characterization of blended filaments

The thermal properties of the PLA/PCL filaments were analyzed using thermogravimetric analysis (TGA; TA SDT 650 instrument). Approximately 10 mg of each sample was placed in a ceramic crucible and heated from room

Table 1: PLA/PCL compositions used in the study

Material	Composition (wt%)	
	PLA	PCL
PLA	100	00
70/30	70	30
50/50	50	50
30/70	35	70
PCL	00	100

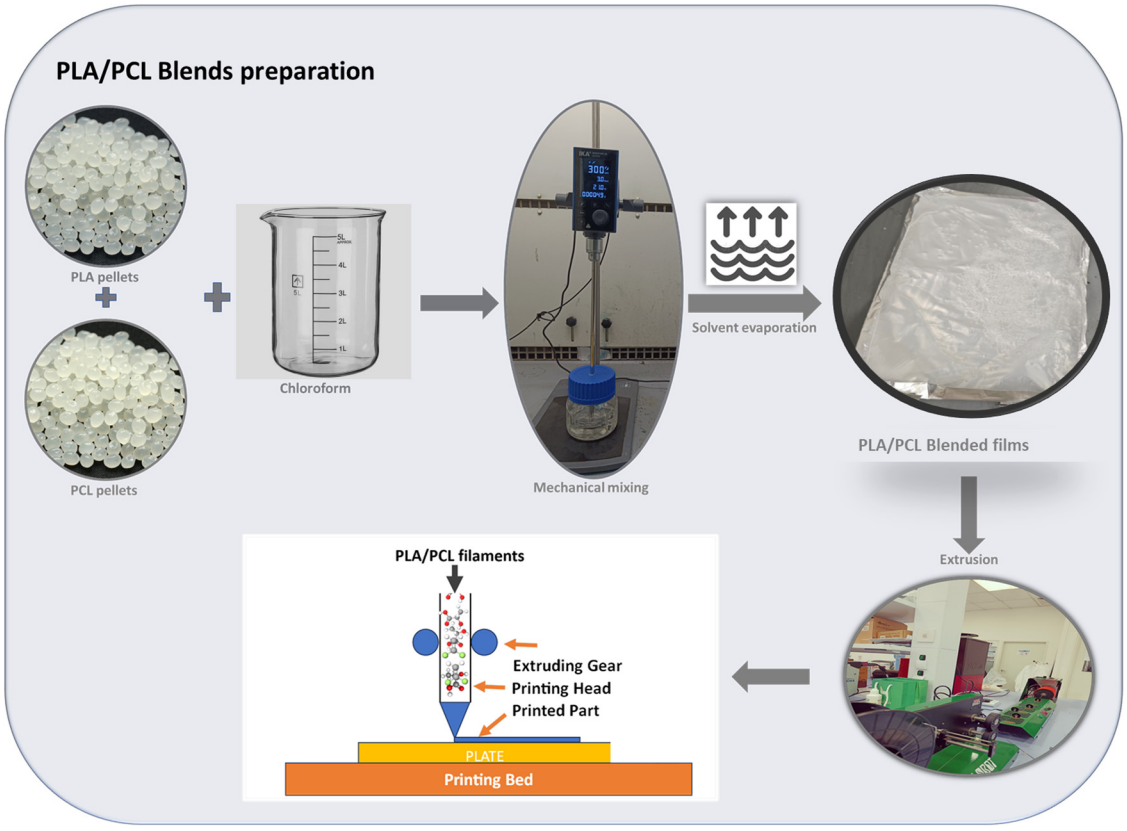

Figure 1: Schematic of the preparation process of PLA/PCL blended filaments for 3DP.

temperature to 500°C at a rate of 10°C per minute under a nitrogen purge. Differential scanning calorimetry (DSC) provided data on the melting and degradation temperatures. X-ray diffractometry was performed to examine the crystal structures over a 10°–90° angle range, and Fourier transform infrared(FTIR) spectroscopy was performed to identify the functional groups, employing an attenuated total reflectance (ATR) attachment and recording transmittance spectra across 4,000–400 cm^{-1} at a 4 cm^{-1} spectral resolution using 32 scans per sample.

2.5 3DP of PLA/PCL filaments

Samples were printed on an Ultimaker 3 Extended FFF printer using the filaments. The solid samples and the tensile test samples were designed using Solidworks and prepared for printing with Ultimaker Cura. The printer settings included a layer resolution of 0.2 mm, and nozzle diameter of 0.4 mm, and 100% infill density. The bottom and top layers were set at 3 each, and the perimeter wall line counts were set at 2. The extrusion temperature, print speed, and bed temperature varied based on the PLA/PCL blend composition. To aid adhesion, paper glue was applied to the build plate.

2.6 Mechanical and degradation studies

Mechanical properties were evaluated using a MARK-10 (ESM303) testing machine. Tensile tests (ASTM D638 Type IV) were performed at an extension rate of 5 $mm{\cdot}min^{-1}$ for three samples of each composition, from which the maximum tensile stress and Young's modulus were calculated. Degradation studies involved immersing 3D-printed solid samples in phosphate-buffered saline (PBS) for 4 weeks, with initial and subsequent weights measured at 2-week intervals. Samples were dried post-immersion before weighing to calculate the percentage of weight loss. For the degradation study, printed samples were first weighed and then placed in glass test tubes filled with 10 mL of PBS. The chemical composition and changes in the functional groups of the PLA/PCL blends were analyzed using an (FTIR spectrometer, both before and after degradation in the PBS solution. To evaluate the degradation of the PLA/PCL scaffolds, they were submerged in a PBS solution with an initial pH of 7.6 for 4

weeks. The reduction in weight of the scaffolds was assessed after weeks 2 and 4. Each scaffold's weight was recorded prior to immersion in PBS. At the 2- and 4-week marks, the samples were removed from the PBS, dried at 40°C for 8 h, and then reweighed. The percentage of weight loss (W%) was calculated using the following formula:

$$\Delta W\% = (W_i - W_f)/W_i \times 100\%,$$

where W_i represents the original weight of the dry, deteriorated scaffolds, and W_f denotes their final weights after degradation.

Additionally, the chemical states of the blended PLA/PCL samples were analyzed both before and after aging, utilizing X-ray photoelectron spectroscopy (XPS)(ESCALAB 250Xi, Thermo Fisher Scientific, UK). The spectroscopic settings for XPS included 20 eV for high-resolution scans and 100 eV for survey scans. The XPS instrument was regularly calibrated with high purity standards of gold (Au), silver (Ag), and copper (Cu). The referencing for these samples was performed using the C1s peak at 284.8 eV.

2.7 Statistical analysis

The data collection was repeated three times to ensure reliability. Results are presented as mean values with standard deviations, illustrating the reproducibility of the findings.

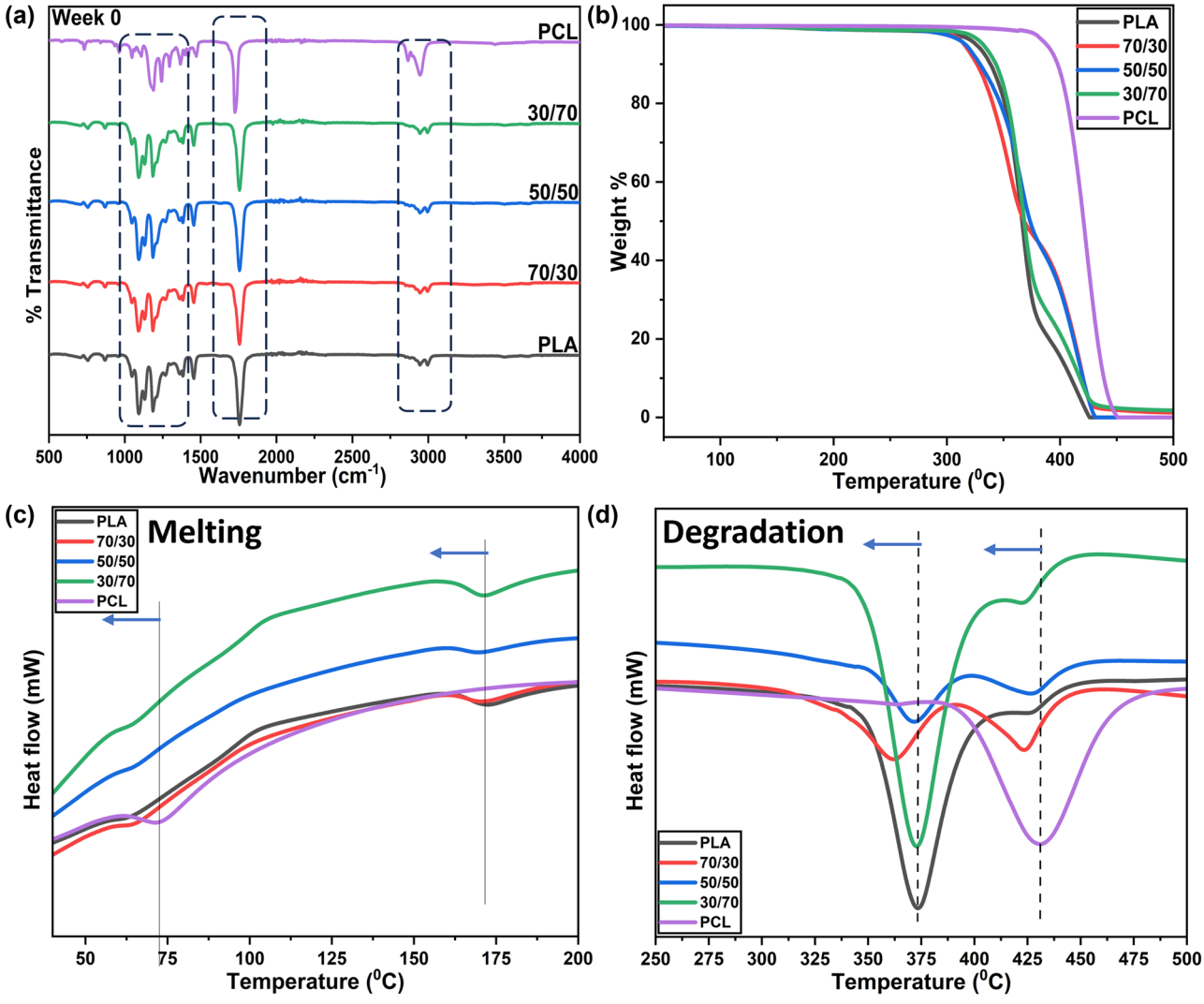

Figure 2: (a) FTIR analysis of the blend, PCL, and pure PLA films. (b) TGA characterization of PLA and blend films. (c) DSC characterization of PLA/PCL blends film in the melting temperature range. (d) DSC characterization of PLA/PCL blend film in the degradation temperature range.

3 Results and discussion

3.1 FTIR spectroscopy results

FTIR spectroscopy is used to determine the chemical functional groups present in a substance. The FTIR spectra of the PLA/PCL blend, shown in Figure 2a, demonstrate the absorption bands of the functional groups that are present in the composite. The FTIR spectra display the following distinctive PLA peaks: bands attributed to the C–O stretching between 1,100 and 1,200 cm^{-1}; bands attributed to C–H bending between 1,325 and 1,500 cm^{-1}; a C═O stretch at 1,757 cm^{-1}, and a small C–H vibration between 2,900 and 3,025 cm^{-1}. The FTIR spectra of pure PCL show the following major distinctive bands at 2,866 and 2,948 cm^{-1} corresponding to the C–H stretching. The presence of this distinctive band of PCL is evident in the PLA/PCL samples, but it has lesser intensity.

Because the chemical functional groups found in PCL and PLA are so similar, the IR bands of blended scaffolds greatly overlap. Furthermore, no new absorption peaks appeared, and no changes to the peak positions were observed. These results show that both polymers mixed nicely in the fibers; nevertheless, during the blending and subsequent extrusion process, there was no chemical contact between the PLA and PCL polymers. The slight variations between PCL and PLA blends imply that the chemical connections were comparable and in line with previous research [28]. The blended peak positions of the two polymers exhibit a small movement in the C–H stretch but otherwise remain mostly unchanged. The peak intensity was, however, slightly decreased.

3.2 Thermal degradation behavior

The weight loss that results from thermal decomposition, the decomposition temperature of a material, and its thermal stability are all frequently ascertained using TGA. TGA can be used to ascertain the temperature at which PLA begins to degrade as well as the degree of degradation that occurs at various temperatures. Additional TGA studies were carried out to determine the limitations in extrusion and printing temperatures as well as the thermal degradation behavior of the produced materials. Up to about 300°C, none of the samples significantly changed in weight, and PCL remained steady even at 400°C. As shown in Figure 2b, pure and blend samples are degraded in a single-step degradation process. PLA degrades thermally between 300°C and 370°C, whereas PCL degrades between 350°C and 450°C. PLA/PCL blends degrade between these two pure polymer degradation temperature ranges. PCL addition speeds up heat breakdown in the PLA [29,30]. The temperature at which 5% of the sample begins to degrade in the blends is higher than that for the pure PLA, showing that the PCL addition increases the thermal stability of the PLA.

DSC measurements were taken to examine the thermal behavior of PLA/PCL blends in the processed blends. The thermal events observed during the DSC analysis are primarily associated with the melting, crystallization, and glass transition behaviors of PLA and PCL. All blends presented a melting peak for PCL at around 55°C, while the melting peak for PLA was observed at 175°C (Figure 2c). Because it overlaps with the melting temperature of PCL, the T_g of the pure PLA looks to be approximately 60°C, making it challenging to determine it during heating scans for blends. The addition of PCL into the PLA matrix led to peaks at both temperatures associated with the polymers. The degradation of the blends also shows a similar trend (Figure 2d). These mechanisms differ due to the inherent structural and thermal properties of the two polymers. The observed differences in these events arise from the distinct thermal and molecular characteristics of PLA and PCL, as well as their interactions in the composite. These mechanisms collectively govern the processability and thermal behavior of the blends, which are critical for their application in 3D-printed scaffolds. The onset of the degradation appears to be quicker with the increasing composition of PLA. The presence of PCL has led to the degradation of the blends to a higher temperature. This shows that the thermal stability of the blends increased with the addition of PCL. This is important to remember when developing materials for biomedical applications since changes in the chemical composition could have detrimental consequences on the body, such as strong immunological reactions.

3.3 3DP of various PLA/PCL blends

Samples of the various PLA/PCL compositions were 3D printed to assess whether filaments are suitable for producing complex geometrical features and whether they can preserve structural integrity during the printing process. It was observed that 3DP of PCL and PLA required different printing parameters. PLA, having a melting temperature of 175°C, showed good printability at a nozzle temperature of 190°C. PCL, which has a melting temperature of around 60°C, could be printed only at around 160°C nozzle temperature. This is due to the variations in MFR of various polymers at different temperatures [31,32].

Table 2: Optimized printing parameters of the blends

	Nozzle temperature (°C)	Printing speed ($mm \cdot s^{-1}$)	Print bed temperature (°C)
PLA	190	50	60
70/30	190	50	40
50/50	190	20	40
30/70	190	20	40
PCL	160	20	40

The printing parameters were selected based on analyzing the melt flow behavior of the PLA/PCL blends through the nozzle at different temperatures and print speeds. The optimal nozzle temperature and print speed were determined by studying the flow characteristics to ensure smooth extrusion and consistent layer deposition for each blend. Additionally, the bed temperature was chosen by evaluating the temperature at which the blends adhered effectively to the print bed and retained their shape during the printing process. This systematic approach ensured the best printing conditions for each PLA/PCL ratio.

The relative proportions of PLA and PCL in the blend impact the MFR. PLA typically has a higher MFR than PCL. As the percentage of PLA increased in the blend, the overall MFR of the blend may tend to increase due to the dominance of PLA's higher MFR [33]. MFR affects how easily the blend material can be extruded through the 3D printer's nozzle [34]. A higher MFR indicates better flowability, leading to smoother and more consistent extrusion. A higher MFR often correlates with improved printability, especially when using smaller nozzle sizes. Therefore, the printing of blends with increasing PCL composition required a much slower print speed for proper deposition of the molten layer (Table 2).

Various optimized print parameters are shown in Table 3. All blend filaments were discovered to be easily printable and free of any flaws or irregularities. Figure 3 illustrates how the printed components adhered to the input design specifications without materially deviating from the original CAD file.

3.4 Degradation study of the 3D printed samples

It is reported in the literature that PCL degrades by scission of end groups of the polymer chain, which disappears when washed and dried [35]. PLA degrades by chain scission, but these chains remain. Blend PLA/PCL scaffolds show intermediate behavior, with each homopolymer degrading following the same mechanism as pristine homopolymers. Figure 4a and b show the FTIR spectra before and after degradation of 4 weeks of the PLA/PCL samples for comparison. The FTIR spectra show degradation of polymer chains after 4 weeks of degradation, which is evident from peaks with lesser intensities compared to the non-degraded sample peaks. The 50/50 PLA/PCL spectra confirm slow degradation due to PCL addition, with the carbonyl band of PLA decreasing faster than PCL [36]. It can be observed from the spectra that there is a broadening of C–H stretches in all the compositions. The appearance of broad O–H stretches in the PCL sample indicates that hydrolytic degradation is prominent in PCL, as shown in the figure.

The weight loss in PLA/PCL blends in PBS is observed over 4 weeks, with a decreasing trend as PCL content increases (Figure 4c). For example, scaffolds with higher PLA content may be more suitable for applications requiring rapid degradation and faster tissue ingrowth, such as in temporary implants for soft tissue repair. On the other hand, scaffolds with higher PCL content provide prolonged structural support in load-bearing applications or in cases where slower degradation is needed to allow sufficient time for tissue regeneration. This ability to customize the degradation profile is particularly beneficial for creating patient-specific solutions, where the scaffold's degradation kinetics can be matched with the healing process of the targeted tissue. The decreasing trend in weight loss with increasing PCL content suggests that the rate of degradation in PBS decreases as more PCL is incorporated into the blend. PLA is known for its relatively rapid biodegradation, whereas PCL has a slower degradation rate. As PCL content increases,

Table 3: XPS spectra details

Sample	Chemical state	Peak BE (eV)	FWHM (eV)	Area (CPS·eV)	Percentage (%)
Non-degraded	C1s (C–C/C–H)	284.82	1.34	71699.03	50.84
	C1s (C–O)	286.79	1.40	36169.70	25.66
	C1s (O–C═O)	288.92	1.25	33116.38	23.50
Degraded	C1s (C–C/C–H)	284.88	1.31	77505.09	47.93
	C1s (C–O)	286.82	1.44	44433.06	27.49
	C1s (O–C═O)	288.93	1.19	39697.93	24.57

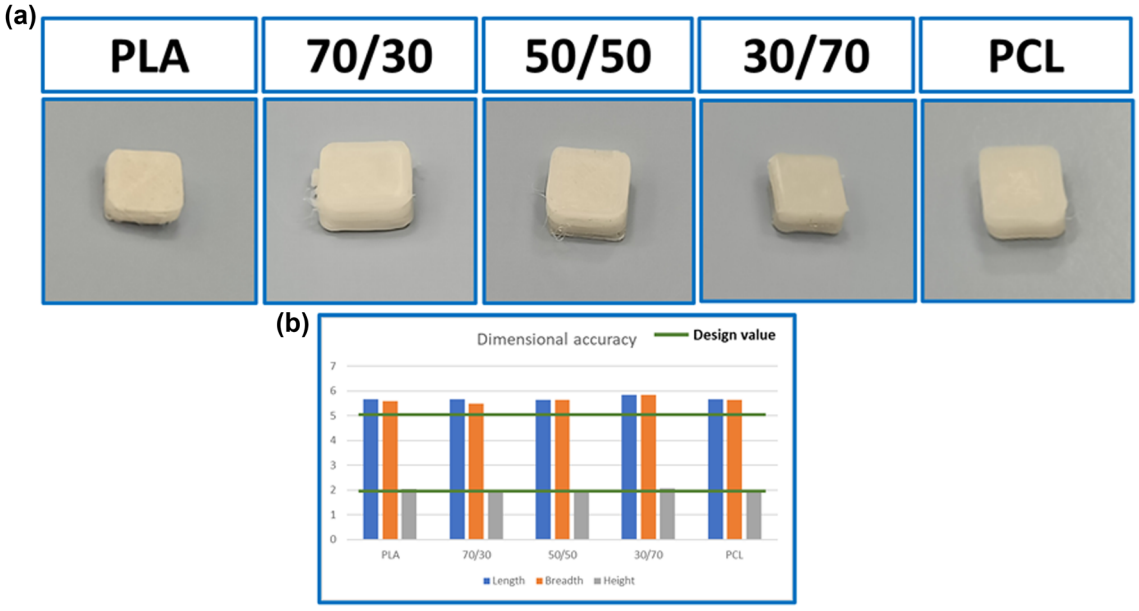

Figure 3: (a) Samples of various compositions prepared using FFF. (b) Plot showing the variation of dimensional accuracy with respect to various compositions.

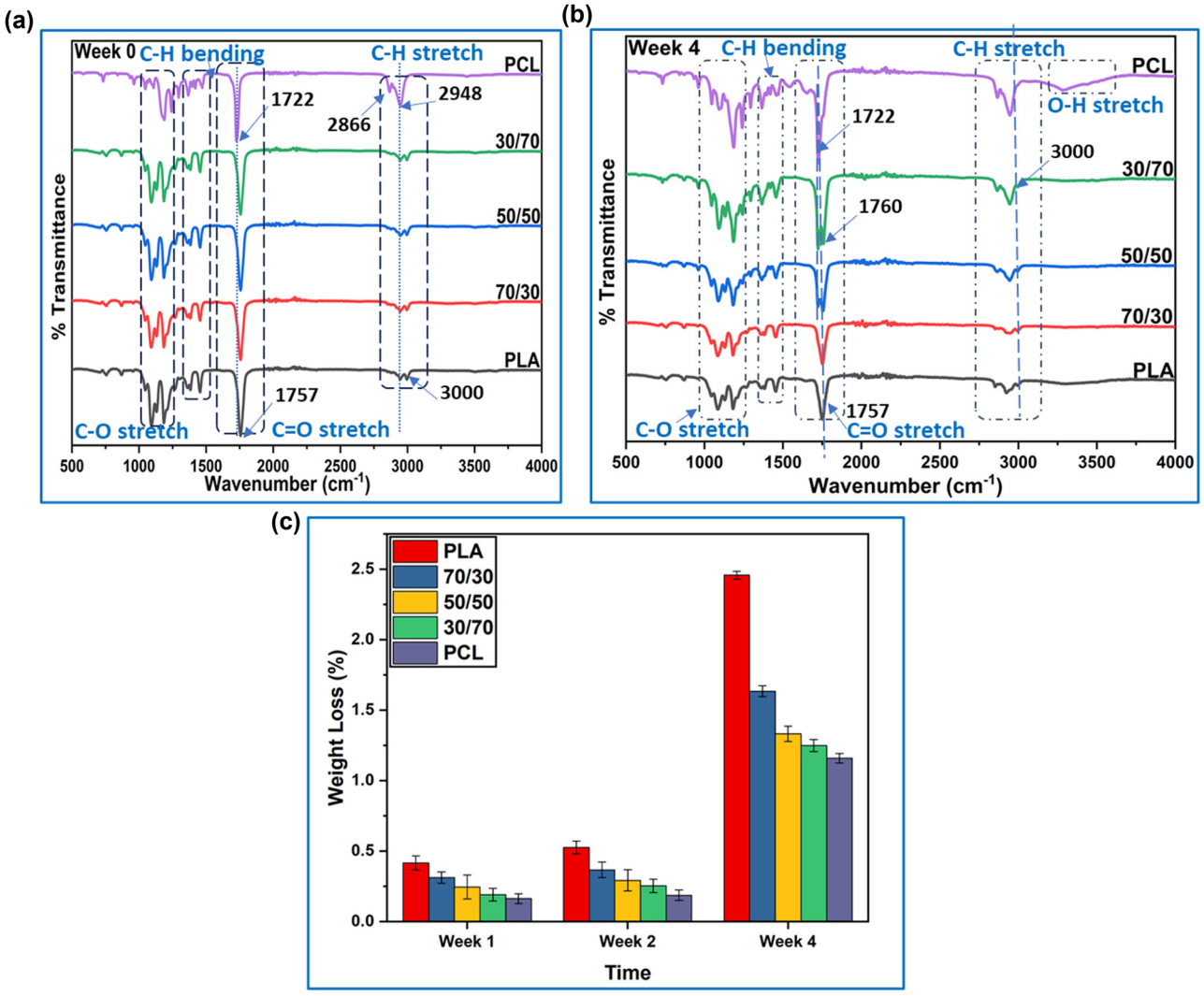

Figure 4: Degradation study results: (a) FTIR results of non-degraded samples, (b) FTIR results of degraded samples, and (c) plot showing the weight loss of the samples after different degradation intervals.

the dominance of PCL in the blend can slow down the overall degradation process [37].

X-ray photoelectron spectroscopy (XPS) is a valuable analytical technique for investigating the degradation of PLA/PCL blend materials. When examining such blends after degradation, XPS results can provide insights into the chemical changes occurring at the material's surface, which is crucial for understanding the degradation mechanisms [38]. An increase in the oxygen concentration at the blend's surface can indicate oxidative degradation. XPS can quantify changes in the oxygen content and help identify the formation of oxygen-containing functional groups, such as carbonyl or hydroxyl groups, which are often associated with the degradation processes.

The mixed PLA/PCL sample before and after degradation has shown that the surface elements are mainly C and O due to the composition of the polymers PLA and PCL. The chemical state analysis indicates that carbon, which is the main element, is present as C–C/C–H, C═O, and O–C═O. Theoretically, PLA has the chemical formula of $(C_3H_4O_2)_n$, which consists of one (1) C–C/C–H, one (1) C–O, and one (1) O–C═O and PCL chemical formula is $(C_6H_{10}O_2)_n$, which has

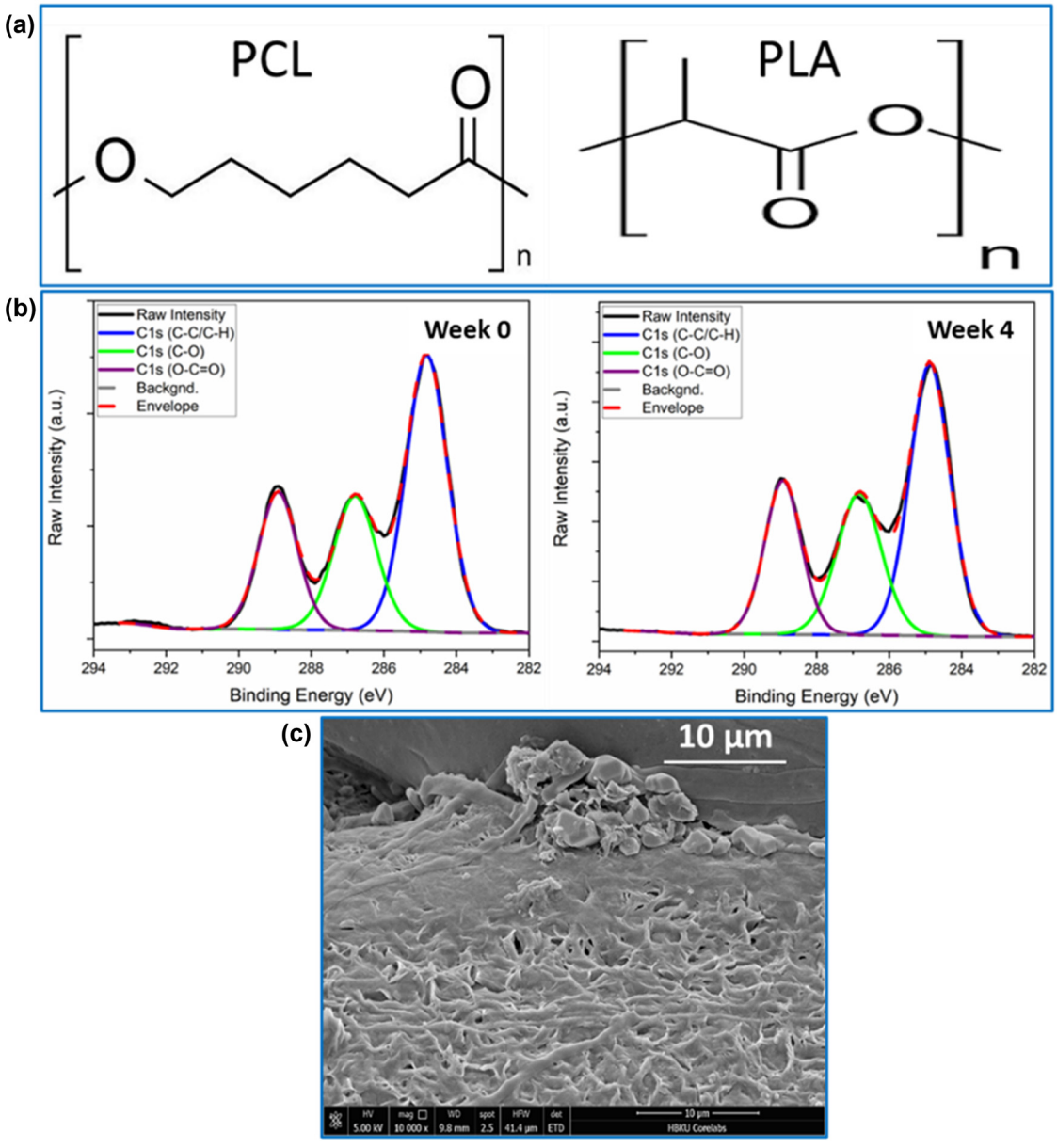

Figure 5: (a) Chemical structure of PCL and PLA monomers, (b) XPS spectra of non-degraded and degraded PLA/PCL 30/70 sample, and (c) SEM of the degraded sample.

four (4) C–C/C–H, one (1) C–O, and one (1) O–C═O, as shown in Figure 5a. Regardless of the mixture, the ratio of C–O to O–C═O should be close to 1:1.

The fresh sample shows a ratio close to 1:1 for C–C/C–H to O–C═O, which is expected (Figure 5b). A ratio of C–C/C–H to C–O and between C–C/C–H and C–O (as well as O–C═O) is close to 2:1, which is related to the mixture of both polymers (Table 3). Abudula *et al.* made similar observations regarding ratios of C–C/C–H to C–O in their study of PLA/PBS hybrid fibers [39]. After the degradation, the C–C/C–H bonds were reduced while the C–O and O–C═O bonds increased. This is likely due to the slight deterioration of the polymer and increased oxidation caused by the hydrolysis of esters (Figure 5c). Similar SEM results for degradation after 4 weeks have been reported in the literature [40].

3.5 Mechanical properties of the 3DP PLA/PCL blends

Natural tissues have a specific mechanical strength and stiffness that allows them to withstand various mechanical loads, provide support, and resist fractures. To design effective tissue engineering scaffolds or implants, it is crucial to match or closely mimic the mechanical properties of the targeted tissues. Mechanical strength studies help ensure that the engineered tissue constructs can provide the required support and resist failure under physiological loads. The results of the tensile tests on PLA/PCL blends are displayed in Figure 6. The stress–strain curves demonstrate a decreasing elastic modulus, decreasing breaking stress, and increasing ductility with increased PCL content. All

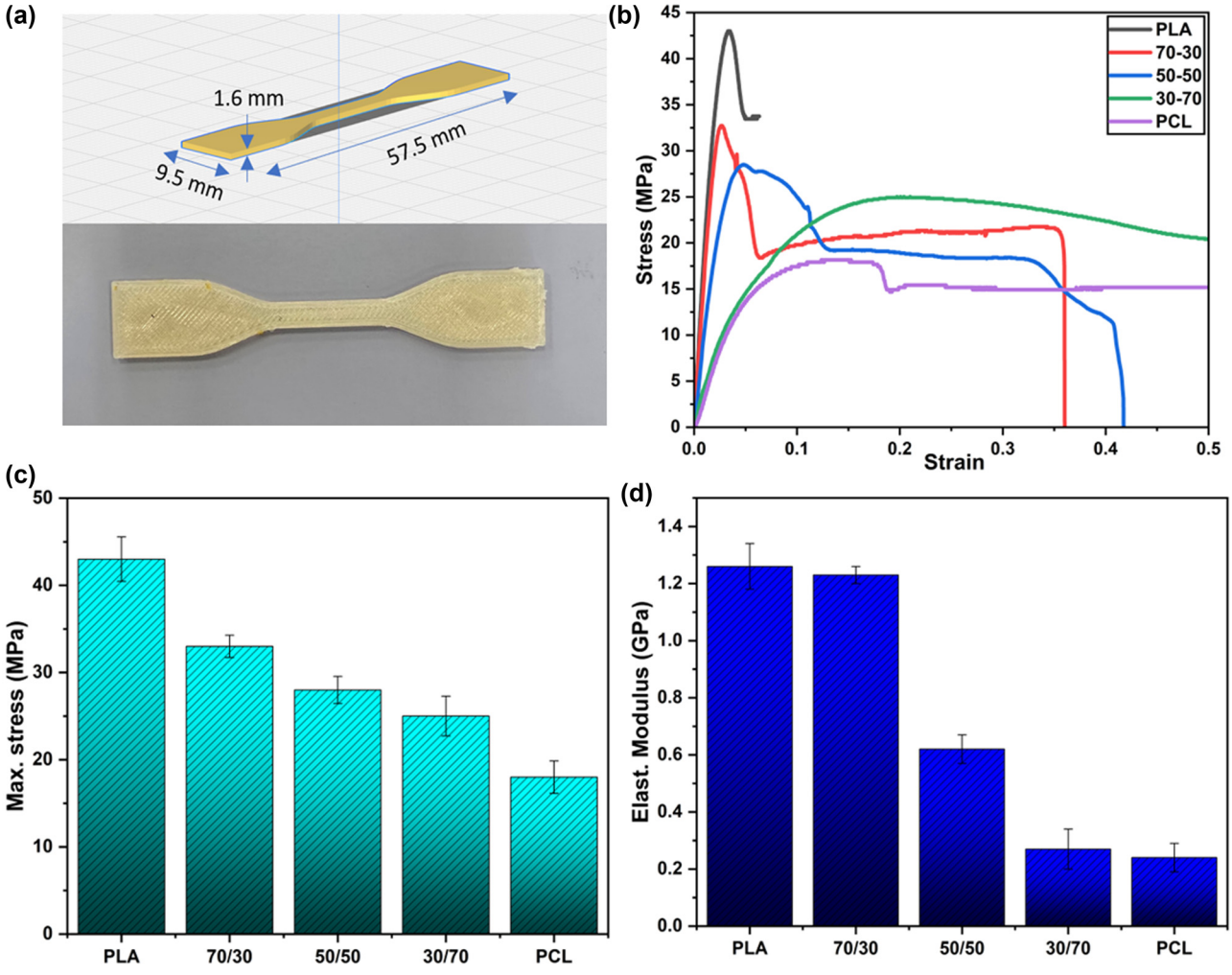

Figure 6: Mechanical study results: (a) Dog-bone samples as per ASTM D638 Type IV. (b) Tensile stress–strain curve of the various PLA/PCL blends. (c) Plot showing the variation of stiffness among the various samples under study. (d) Plot showing the variation of maximum stress among the various samples under study.

Table 4: Mechanical properties of the blends

	Max. stress (MPa)	Elastic modulus, *E* (GPa)	Elongation at break (%)
PLA	43 ± 2.54	1.26 ± 0.08	5
70/30	33 ± 1.28	1.23 ± 0.03	35
50/50	28 ± 1.56	0.62 ± 0.05	42
30/70	25 ± 2.28	0.27 ± 0.07	>50
PCL	18 ± 1.86	0.24 ± 0.05	>50

the mechanical properties of the blends are tabulated in Table 4. As seen in the tensile stress–strain plot, 100% PCL reaches the highest value of maximum elongation at break, while 100% PLA reaches higher stress values. The three blend blends exhibit in between these behaviors.

Breaking stress, often called tensile strength, is the maximum stress a material can withstand before rupturing. PLA typically has a higher tensile strength compared to PCL [41]. With an increase in the PCL content, the overall strength of the blend decreases. This can be attributed to PCL being a weaker polymer in tensile strength. Pure PLA exhibits the highest breaking stress (43 MPa) among the tested materials. This is consistent with the reputation of PLA for its good mechanical strength. The PLA/PCL blend (70/30) retained a relatively high breaking stress (33 MPa) compared to the other blends. This demonstrates that even with significant PCL addition, the material maintains a substantial level of strength. Pure PCL exhibits the lowest breaking stress (18 MPa) among the tested materials. PCL is known for its lower strength compared to PLA [42]. The breaking stress values of the blends, especially those with higher PLA content, approach the lower range of breaking stress observed in bones.

The elastic modulus (or Young's modulus) measures a material's stiffness and resistance to deformation. PLA is known for its relatively high modulus, whereas PCL has a lower modulus. The overall stiffness decreases as the PCL content increases in the blend. This is expected because PCL is a more flexible and less stiff polymer compared to PLA. Pure PLA has the highest elastic modulus (1.26 GPa), indicating its stiffness and resistance to deformation. This is consistent with the reputation of PLA as a relatively stiff polymer [31]. The blend with 70% PLA content maintains a high elastic modulus (1.23 GPa), indicating that it retains stiffness even with a significant PCL component. Pure PCL has the lowest elastic modulus among the tested materials, indicating its flexibility and lower stiffness. Lower PLA content blends offer a balance between stiffness and strength, which can be advantageous in applications where controlled mechanical properties are needed.

Ductility refers to a material's ability to undergo plastic deformation (change in shape) without fracturing. PLA is known for its brittleness, which tends to fracture without significant plastic deformation. On the other hand, PCL is more ductile. When PCL is incorporated into the blend, it imparts greater ductility to the material. Pure PLA exhibits the lowest elongation at break (5%), indicating its brittleness. PLA tends to fracture without significant plastic deformation. A blend with 70% PLA content significantly improves elongation at break (35%), suggesting increased ductility compared to pure PLA. The elongation at break exceeds 50% with a lower PLA content, indicating a highly ductile material. The elongation at break results reveals that PCL-based blends and those with lower PLA content are highly ductile. This ductility can be advantageous in applications where flexibility and resistance to fracture are crucial [43,44].

PLA and PCL have different chemical structures and properties. The observed changes in the mechanical properties may be influenced by the compatibility of these polymers at the molecular level. Poor compatibility can lead to weak interfacial bonding between the two components, reducing the overall mechanical performance. The distribution and alignment of PLA and PCL phases within the blend can affect the mechanical properties. If PCL domains are well dispersed and aligned, it can increase ductility and decrease stiffness and strength. The ability to tune the mechanical properties of PLA/PCL blends by adjusting the PCL content provides opportunities to tailor materials for specific applications [32,45]. For instance, a higher PCL content might be desirable in applications where flexibility and impact resistance are crucial. These findings open opportunities for tailoring materials with specific mechanical properties, making them suitable for various applications, particularly biodegradable and sustainable materials. The decreasing elastic modulus of PLA/PCL blends with increasing PCL content can benefit bone tissue engineering. Human bones have some flexibility, and excessively stiff materials may not integrate well with the surrounding bone tissue [46–48]. The increased ductility in PLA/PCL blends is particularly beneficial in load-bearing bone tissue engineering applications. Bones are subjected to dynamic loads, and materials with some ductility can better withstand these mechanical stresses without fracturing. This property is critical for long-term implant durability (Figure 6).

4 Conclusion

This study investigated the potential of PLA/PCL blends as FFF feedstock for bone tissue engineering applications. The

results demonstrated that the mechanical properties of the blends can be tailored by adjusting the composition ratio of PLA and PCL, enabling the fabrication of structures according to patient-specific requirements. In summary, the observed mechanical property trends in PLA/PCL blends, including decreasing stiffness, increasing ductility, and biodegradability, align well with the requirements for bone tissue engineering applications. These blends can potentially contribute to the development of advanced biomaterials for bone repair and regeneration, offering customizable solutions for a range of clinical scenarios. Further research, including *in vitro* and *in vivo* studies, will be necessary to validate their suitability and optimize their performance for specific bone tissue engineering applications. Further research and optimization are warranted to explore their long-term performance, integration with vascularization strategies, and translation into clinical practice.

Acknowledgments: The authors acknowledge the contributions of the HBKU core labs for the support provided in the characterization of the samples.

Funding information: The authors acknowledge the partial support by QNRF through project NPRP13S-0126-200172 (Additive Manufacturing of Mg-based Porous Tissue Scaffolds). Open Access funding is provided by the Qatar National Library.

Author contributions: All authors have accepted responsibility for the entire content of this manuscript and given consent to its submission to the journal, reviewed all the results, and approved the final version of the manuscript. MK and CA designed the experiments, and SN performed them. YZ performed the XPS study and analyzed the results. SN prepared the manuscript with contributions from all coauthors. All authors have accepted responsibility for the entire content of this manuscript and approved its submission.

Conflict of interest: The authors state no conflict of interest.

Data availability statement: The datasets generated and/or analyzed during the current study are available from the corresponding author on reasonable request.

References

[1] Hutmacher, D. W. Scaffolds in tissue engineering bone and cartilage. *Biomaterials*, Vol. 21, 2000, pp. 2529–2543.

[2] Prabhakaran, M. P., J. Venugopal, and S. Ramakrishna. Electrospun nanostructured scaffolds for bone tissue engineering. *Acta Biomaterialia*, Vol. 5, 2009, pp. 2884–2893.

[3] Sheikh, Z., S. Najeeb, Z. Khurshid, V. Verma, H. Rashid, and M. Glogauer. Biodegradable materials for bone repair and tissue engineering applications. *Materials*, Vol. 8, 2015, pp. 5744–5794.

[4] Kraus, T., S. F. Fischerauer, A. C. Hänzi, P. J. Uggowitzer, J. F. Löffler, and A. M. Weinberg. Magnesium alloys for temporary implants in osteosynthesis: in vivo studies of their degradation and interaction with bone. *Acta Biomaterialia*, Vol. 8, 2012, pp. 1230–1238.

[5] Rahman, M., N. K. Dutta, and N. Roy Choudhury. Magnesium alloys with tunable interfaces as bone implant materials. *Frontiers in Bioengineering and Biotechnology*, Vol. 8, 2020, id. 564.

[6] Khoo, L. K., S. Kiattavorncharoen, V. Pairuchvej, N. Lakkhanachatpan, N. Wongsirichat, and D. Seriwatanachai. The affinity of human fetal osteoblast to laser-modified titanium implant fixtures. *The Open Dentistry Journal*, Vol. 14, 2020, pp. 52–58.

[7] Singh, D., R. Singh, K. S. Boparai, I. Farina, L. Feo, and A. K. Verma. In-vitro studies of SS 316 L biomedical implants prepared by FDM, vapor smoothing and investment casting. *Composites Part B: Engineering*, Vol. 132, 2018, pp. 107–114.

[8] Muley, S. V., A. N. Vidvans, G. P. Chaudhari, and S. Udainiya. An assessment of ultra fine grained 316L stainless steel for implant applications. *Acta Biomaterialia*, Vol. 30, 2016, pp. 408–419.

[9] Xiang, D. D., P. Wang, X. P. Tan, S. Chandra, C. Wang, M. L. S. Nai, et al. Anisotropic microstructure and mechanical properties of additively manufactured Co–Cr–Mo alloy using selective electron beam melting for orthopedic implants. *Materials Science and Engineering: A*, Vol. 765, 2019, id. 138270.

[10] Kalva, S. N., Y. B. Dalvi, N. Khanam, R. Varghese, I. Ahammed, R. Augustine, et al. Air-jet spun PHBV/PCL blend tissue engineering scaffolds exhibit improved mechanical properties and cell proliferation. *Results in Materials*, Vol. 19, 2023, id. 100415.

[11] Yousaf, A., A. Al Rashid, R. Polat, and M. Koç. Potential and challenges of recycled polymer plastics and natural waste materials for additive manufacturing. *Sustainable Materials and Technologies*, Vol. 41, 2024, id. e01103.

[12] Ali, F., S. N. Kalva, and M. Koc. Advancements in 3D printing techniques for biomedical applications: a comprehensive review of materials consideration, post processing, applications, and challenges. *Discover Materials*, Vol. 4, 2024, id. 53.

[13] Kalva, S. N., F. Ali, C. A. Velasquez, and M. Koç. 3D-Printable PLA/Mg composite filaments for potential bone tissue engineering applications. *Polymers*, Vol. 15, 2023, id. 2572.

[14] Augustine, R., S. N. Kalva, Y. B. Dalvi, R. Varghese, M. Chandran, and A. Hasan. Air-jet spun tissue engineering scaffolds incorporated with diamond nanosheets with improved mechanical strength and biocompatibility. *Colloids and Surfaces B, Biointerfaces*, Vol. 221, 2023, id. 112958.

[15] Ali, F., S. N. Kalva, K. H. Mroue, K. S. Keyan, Y. Tong, O. M. Khan, et al. Degradation assessment of Mg-Incorporated 3D printed PLA scaffolds for biomedical applications. *Bioprinting*, Vol. 35, 2023, id. e00302.

[16] Malikmammadov, E., T. E. Tanir, A. Kiziltay, V. Hasirci, and N. Hasirci. PCL and PCL-based materials in biomedical applications. *Journal of Biomaterials Science, Polymer Edition*, Vol. 29, 2018, pp. 863–893.

[17] Patrício, T., M. Domingos, A. Gloria, U. D'Amora, J. F. Coelho, and P. J. Bártolo. Fabrication and characterisation of PCL and PCL/PLA scaffolds for tissue engineering. *Rapid Prototyping Journal*, Vol. 20, 2014, pp. 145–156.

[18] Nuthana Kalva, S., F. Ali, K. Subhadra Keyan, O. M. Khan, M. Pasha, C. A. Velasquez, et al. Effect of Mg incorporation on the properties

of PCL/Mg composites for potential tissue engineering applications. *Frontiers in Materials*, Vol. 11, 2024, id. 1294811.

[19] Arif, Z. U., M. Y. Khalid, R. Noroozi, A. Sadeghianmaryan, M. Jalalvand, and M. Hossain. Recent advances in 3D-printed polylactide and polycaprolactone-based biomaterials for tissue engineering applications. *International Journal of Biological Macromolecules*, Vol. 218, 2022, pp. 930–968.

[20] Joseph, T. M., A. Kallingal, A. M. Suresh, D. K. Mahapatra, M. S. Hasanin, J. Haponiuk, et al. 3D printing of polylactic acid: recent advances and opportunities. *The International Journal of Advanced Manufacturing Technology*, Vol. 125, 2023, pp. 1015–1035.

[21] Wang, X., L. Huang, Y. Li, Y. Wang, X. Lu, Z. Wei, et al. Research progress in polylactic acid processing for 3D printing. *Journal of Manufacturing Processes*, Vol. 112, 2024, pp. 161–178.

[22] Arif, Z. U., M. Y. Khalid, R. Noroozi, M. Hossain, H. H. Shi, A. Tariq, et al. Additive manufacturing of sustainable biomaterials for biomedical applications. *Asian Journal of Pharmaceutical Sciences*, Vol. 18, 2023, id. 100812.

[23] Matta, A. K., R. U. Rao, K. N. S. Suman, and V. Rambabu. Preparation and characterization of biodegradable PLA/PCL polymeric blends. *Procedia Materials Science*, Vol. 6, 2014, pp. 1266–1270.

[24] Navarro-Baena, I., V. Sessini, F. Dominici, L. Torre, J. M. Kenny, and L. Peponi. Design of biodegradable blends based on PLA and PCL: From morphological, thermal and mechanical studies to shape memory behavior. *Polymer Degradation and Stability*, Vol. 132, 2016, pp. 97–108.

[25] Caminero, M. Á., J. M. Chacón, E. García-Plaza, P. J. Núñez, J. M. Reverte, and J. P. Becar. Additive manufacturing of PLA-based composites using fused filament fabrication: effect of graphene nanoplatelet reinforcement on mechanical properties, dimensional accuracy and texture. *Polymers*, Vol. 11, 2019, id. 799.

[26] Sabalina, A., S. Gaidukovs, M. Jurinovs, L. Grase, and O. Platnieks. Fabrication of poly(lactic acid), poly(butylene succinate), and poly (hydroxybutyrate) bio-based and biodegradable blends for application in fused filament fabrication-based 3D printing. *Journal of Applied Polymer Science*, Vol. 140, 2023, id. e54031.

[27] Kalva, S. N., F. Ali, C. A. Velasquez, and M. Koç. 3D-Printable PLA/Mg composite filaments for potential bone tissue engineering applications. *Polymers*, Vol. 15, 2023, id. 2572.

[28] Antoniac, I., D. Popescu, A. Zapciu, A. Antoniac, F. Miculescu, and H. Moldovan. Magnesium filled polylactic acid (PLA) material for filament based 3D printing. *Materials*, Vol. 12, 2019, id. 719.

[29] Motoyama, T., T. Tsukegi, Y. Shirai, H. Nishida, and T. Endo. Effects of MgO catalyst on depolymerization of poly-l-lactic acid to l,l-lactide. *Polymer Degradation and Stability*, Vol. 92, 2007, pp. 1350–1358.

[30] Ferrández-Montero, A., M. Lieblich, J. L. González-Carrasco, R. Benavente, V. Lorenzo, R. Detsch, et al. Development of biocompatible and fully bioabsorbable PLA/Mg films for tissue regeneration applications. *Acta Biomaterialia*, Vol. 98, 2019, pp. 114–124.

[31] Ostafinska, A., I. Fortelny, M. Nevoralova, J. Hodan, J. Kredatusova, and M. Slouf. Synergistic effects in mechanical properties of PLA/PCL blends with optimized composition, processing, and morphology. *RSC Advances*, Vol. 5, 2015, pp. 98971–98982.

[32] Ostafinska, A., I. Fortelný, J. Hodan, S. Krejčíková, M. Nevoralová, J. Kredatusová, et al. Strong synergistic effects in PLA/PCL blends: Impact of PLA matrix viscosity. *Journal of the Mechanical Behavior of Biomedical Materials*, Vol. 69, 2017, pp. 229–241.

[33] Malinowski, R. Some effects of radiation treatment of biodegradable PCL/PLA blends. *Journal of Polymer Engineering*, Vol. 38, 2018, pp. 635–640.

[34] Wang S., L. Capoen, D. R. D'hooge, L. Cardon. Can the melt flow index be used to predict the success of fused deposition modelling of commercial poly(lactic acid) filaments into 3D printed materials?, *Plastics, Rubber and Composites*, Vol. 47, 2018, pp. 9–16.

[35] Scaffaro, R., F. Lopresti, and L. Botta. Preparation, characterization and hydrolytic degradation of PLA/PCL co-mingled nanofibrous mats prepared via dual-jet electrospinning. *European Polymer Journal*, Vol. 96, 2017, pp. 266–277.

[36] Bartnikowski, M., T. R. Dargaville, S. Ivanovski, and D. W. Hutmacher. Degradation mechanisms of polycaprolactone in the context of chemistry, geometry and environment. *Progress in Polymer Science*, Vol. 96, 2019, pp. 1–20.

[37] Dias, J. R., A. Sousa, A. Augusto, P. J. Bártolo, and P. L. Granja. Electrospun polycaprolactone (PCL) degradation: an in vitro and in vivo study. *Polymers*, Vol. 14, 2022, id. 3397.

[38] Al-Gaashani, R., A. Najjar, Y. Zakaria, S. Mansour, and M. A. Atieh. XPS and structural studies of high quality graphene oxide and reduced graphene oxide prepared by different chemical oxidation methods. *Ceramics International*, Vol. 45, 2019, pp. 14439–14448.

[39] Abudula, T., U. Saeed, N. Salah, A. Memic, and H. Al-Turaif. Study of electrospinning parameters and collection methods on size distribution and orientation of PLA/PBS hybrid fiber using digital image processing. *Journal of Nanoscience and Nanotechnology*, Vol. 18, 2018, pp. 8240–8251.

[40] Gong, M., Q. Zhao, L. Dai, Y. Li, and T. Jiang. Fabrication of polylactic acid/hydroxyapatite/graphene oxide composite and their thermal stability, hydrophobic and mechanical properties. *Journal of Asian Ceramic Societies*, Vol. 5, 2017, pp. 160–168.

[41] Simões, C. L., J. C. Viana, and A. M. Cunha. Mechanical properties of poly (ε-caprolactone) and poly (lactic acid) blends. *Journal of Applied Polymer Science*, Vol. 112, 2009, pp. 345–352.

[42] Ko, J., N. K. Mohtaram, F. Ahmed, A. Montgomery, M. Carlson, P. C. D. Lee, et al. Fabrication of poly (ε-caprolactone) microfiber scaffolds with varying topography and mechanical properties for stem cell-based tissue engineering applications. *Journal of Biomaterials Science, Polymer Edition*, 25, 2014, pp. 1–17.

[43] Santoro, M., S. R. Shah, J. L. Walker, and A. G. Mikos. Poly (lactic acid) nanofibrous scaffolds for tissue engineering. *Advanced Drug Delivery Reviews*, Vol. 107, 2016, pp. 206–212.

[44] Sanchez Diaz, R., J. R. Park, L. L. Rodrigues, P. D. Dalton, E. M. De-Juan-Pardo, and T. R. Dargaville. Highly elastic scaffolds produced by melt electrowriting of poly (L-lactide-co-ε-caprolactone). *Advanced Materials Technologies*, Vol. 7, 2022, id. 2100508.

[45] Patrício, T., M. Domingos, A. Gloria, and P. Bártolo. Characterisation of PCL and PCL/PLA scaffolds for tissue engineering. *Procedia CIRP*, Vol. 5, 2013, pp. 110–114.

[46] Pereira, H. F., I. F. Cengiz, F. S. Silva, R. L. Reis, and J. M. Oliveira. Scaffolds and coatings for bone regeneration. *Journal of Materials Science. Materials in Medicine*, Vol. 31, 2020, pp. 1–16.

[47] Turnbull, G., J. Clarke, F. Picard, P. Riches, L. Jia, F. Han, et al. 3D bioactive composite scaffolds for bone tissue engineering. *Bioactive materials*, Vol. 3, 2018, pp. 278–314.

[48] R. Dwivedi, S. Kumar, R. Pandey, A. Mahajan, D. Nandana, D. S. Katti, et al. Polycaprolactone as biomaterial for bone scaffolds: Review of literature, *Journal of Oral Biology and Craniofacial Research*, Vol. 10, 2020, id. 381.